LATVIAN JOURNAL OF PHYSICS AND TECHNICAL SCIENCES
2016, N 2

DOI: 10.1515/lpts-2016-0011

SOLID STATE PHYSICS

STUDY OF COPPER NITRIDE THIN FILM STRUCTURE

A. Kuzmin, A. Kalinko, A. Anspoks, J. Timoshenko, R. Kalendarev

Institute of Solid State Physics, University of Latvia,
8 Kengaraga Str., Riga, LV-1063, LATVIA
e-mail: a.kuzmin@cfi.lu.lv

X-ray diffraction and x-ray absorption spectroscopy at the Cu K-edge were used to study the atomic structure in copper nitride (Cu_3N) thin films. Textured nanocrystalline films are obtained upon dc magnetron sputtering on substrates heated at about 190 °C, whereas amorphous films having strongly disordered structure already in the second coordination shell of copper are deposited in the absence of heating.

Keywords*: copper nitride, thin film, x-ray diffraction, x-ray absorption spectroscopy.*

1. INTRODUCTION

Copper nitride (Cu_3N) has a cubic anti-ReO_3-type structure (Fig. 1) with the lattice parameter a_0=3.811-3.820 Å and is composed of the NCu_6 octahedra joined by corners [1], [2]. Practical interest in the fabrication of copper nitride has grown in the recent years motivated by its possible applications in the thin film form as a material for write-once read many (WORM) optical storage devices [3], [4], for the fabrication of low-resistance magnetic tunnel junctions for non-volatile magnetic random access memories [5], as promising cathodic electrocatalysts in alkaline fuel cells [6], in optical lithography for fabrication of microscopic metal links [7], [8] and, very recently, as an absorber for photovoltaic and photoelectrochemical solar cells [9], [10].

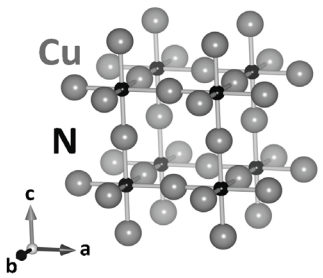

Fig. 1. Crystal structure of cubic (space group *Pm*-3*m*) antiperovskite Cu_3N built up from NCu_6 regular octahedra. Large balls are copper atoms, small balls are nitrogen atoms.

The atomic structure of Cu_3N facilitates anisotropic thermal vibrations of Cu atoms, whose thermal ellipsoids are flattened in the direction perpendicular to the N–Cu–N atomic chains [1], and accepts the presence of nitrogen vacancies or nitrogen/copper interstitial dopants that may result in a variation of the lattice parameter by up to ±0.08 Å [11], [12].

Chemical bonding and electronic properties of Cu_3N are strongly related to its atomic structure. The Cu–N bonds along linear N–Cu–N atomic chains are partially covalent due to an admixture of Cu(4s, 4p) states to the Cu(3d)-N(2p) bands, which do not lead to a covalent energy gain alone [13]. Cu_3N is a narrow band gap (0.25–1.90 eV [10]) semiconductor. However, small changes in the interactions between copper atoms stimulated by the formation of nitrogen vacancies may result in further band gap narrowing or even band overlap [11], because the nearest Cu–Cu distance of about 2.70 Å in Cu_3N is only slightly larger than that of 2.56 Å found in metallic copper. The transition of Cu_3N to metallic state can also be promoted by copper doping [14], [15] or by applying high pressure [16], [17]. Thus, the information on the local atomic structure and disorder in Cu_3N thin films is important for the understanding and tuning of their properties.

In this study, we have performed complementary x-ray diffraction and x-ray absorption spectroscopy investigations of the atomic structure in Cu_3N thin films produced by dc magnetron sputtering as a function of film preparation conditions.

2. EXPERIMENTAL AND DATA ANALYSIS

Polycrystalline Cu_3N thin films were prepared by dc magnetron sputtering of metal copper target in pure N_2 atmosphere on glass and polyimide substrates with average deposition rate of 2.0 nm/sec using modified magnetron sputter deposition system UVN-3. The deposition parameters and thickness of the films are reported in Table 1. The film thickness was measured by profilometer Veeco Dektak 150. Polycrystalline Cu_3N (99.5% purity, AlfaAesar) was used for comparison.

X-ray powder diffraction (XRD) patterns (Fig. 2) were recorded at room temperature (20 °C) using a θ-θ Bragg-Brentano powder diffractometer PANalytical X'Pert Pro MPD, equipped with copper anode x-ray tube (Model PW3373, Cu K_α radiation, λ=0.154 nm).

X-ray absorption measurements were performed at the Cu K-edge (8979 eV) in transmission mode at the HASYLAB/DESY C bending-magnet beamline [18] at room temperature. The storage ring DORIS III operated at E=4.44 GeV and I_{max}=140 mA. The higher order harmonics were reduced by detuning the double-monochromator Si(111) crystals to 60 % of the rocking curve maximum, using the beam-stabilization feedback control. The x-ray beam intensity was measured by ionization chambers filled with argon and krypton gases.

X-ray absorption spectra were analysed using the EDA software package [19]. The extended X-ray absorption fine structure (EXAFS) $\chi(k)$ was isolated following a conventional procedure [20], [21]. The contribution from the first (Cu–N) and second (Cu–Cu) coordination shells was singled out using Fourier filtering procedure in the range of 0.8–3.1 Å and analysed within the single-scattering Gaussian approxi-

mation to determine structural parameters. The self-consistent, real space multiple-scattering FEFF8.2 code [22], [23] was used to generate the backscattering amplitude and phase shift functions for Cu–N and Cu–Cu atom pairs based on crystallographic data of Cu_3N [1]. The complex exchange-correlation Hedin-Lundqvist potential was used to account for inelastic effects. The crystal potential was of muffin-tin (MT) type, and the values of the MT-radii were R_{MT}(Cu)=1.22 Å and R_{MT}(N)=0.97 Å.

Table 1

Thin Film Preparation Conditions, Thickness and Lattice Parameter of Cu_3N Samples

Sample	Deposition time (sec)	Substrate temperature (°C)	Film thickness (nm)	Lattice parameter (Å)
Bulk Cu_3N	-	-	-	3.819
TF1	120	20	229	-
TF2	30	191	74	3.816
TF3	120	196	224	3.796

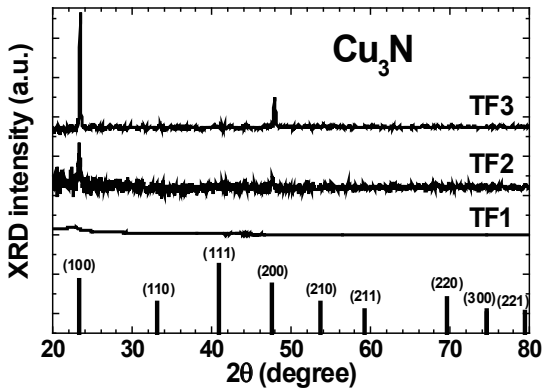

Fig. 2. X-ray diffraction patterns for Cu_3N thin films. Vertical bars show positions of the Bragg peaks for bulk Cu_3N phase (JCPDS No. 47-1088).

3. RESULTS AND DISCUSSION

The thin film TF1 deposited at the substrate temperature of 20 °C is amorphous (Fig. 2), and its XRD pattern originated mainly from the glass substrate. Two other films deposited at the substrate temperatures of 191 °C (TF2) and 196 °C (TF3) are nanocrystalline and strongly textured with crystal growth direction [100]. Their diffraction patterns are indexed to the (100) and (200) planes of cubic Cu_3N. Note that similar preferential growth of Cu_3N along the [100] direction was reported in [11], [24], [25] for films produced by reactive radio-frequency (RF) magnetron sputtering. The lattice parameter a_0 in thin film samples TF2 and TF3 determined from the position of the (100) and (200) peaks is slightly smaller than in bulk Cu_3N (Table 1) that indicates some substoichiometry of the films [11].

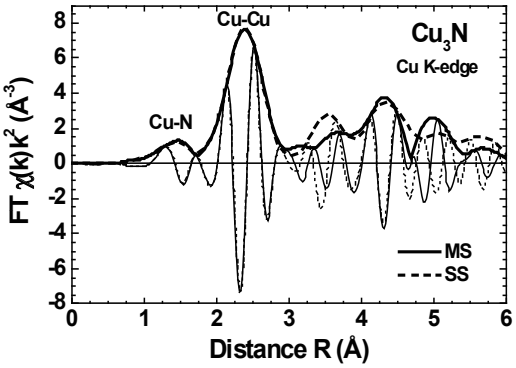

Fig. 3. Fourier transforms (thin lines – imaginary parts and thick lines – moduli) of the calculated Cu K-edge EXAFS $\chi(k)k^2$ for Cu_3N. Solid line – the signal including all multiple-scattering (MS) contributions up to the 6th order, dashed line – the signal including only the single-scattering (SS) contributions. Note that the positions of the peaks differ from the crystallographic values due to the phase shift present in EXAFS.

Table 2

Interatomic Distances (*R*, ±0.01 Å) and Mean-Squared Relative Displacements (σ^2, ±0.0007 Å^2) for Nearest Cu–N and Cu–Cu Atom Pairs Obtained from the Analysis of the Cu K-edge EXAFS Spectra

Sample	Cu–N		Cu–Cu	
	R (Å)	σ^2 (Å^2)	*R* (Å)	σ^2 (Å^2)
Bulk Cu_3N	1.89	0.0022	2.64	0.0130
TF1	1.88	0.0022	2.60	0.0270
TF2	1.90	0.0024	2.67	0.0184
TF3	1.89	0.0026	2.68	0.0158

Since Cu_3N has anti-perovskite type structure with linear Cu–N–Cu atomic chains, one can expect significant contribution of the multiple-scattering (MS) effects [26] into EXAFS. Therefore, we have performed ab initio multiple-scattering calculations by the FEFF8.2 code [22], [23] for bulk Cu_3N to estimate the *R*-space range where such contributions are important. No thermal effects were included into calculations, leading to overestimated peak amplitudes. The obtained results are reported in Fig. 3 and suggest that the first two peaks in Fourier transform (FT) of EXAFS, which correspond to the first (Cu–N atom pair) and second (Cu–Cu atom pair) coordination shells of copper, are free from MS contributions and, thus, can be analysed within the single-scattering (SS) approximation using conventional multicomponent analysis procedure [20], [21]. The analysis of peaks above 3 Å requires inclusion of the MS effects through some sophisticated procedure, as, for example, described in [27], and will not be discussed here.

The shape of the Cu K-edge EXAFS for the films TF2 and TF3 produced on heated substrates is close to that in bulk Cu_3N, except some features are less resolved (Fig. 4). A comparison of their Fourier transforms suggests the nanocrystalline structure of the films appearing as progressive reduction of the amplitude of distant peaks due to a contribution of under-coordinated atoms located at the nanocrystallite surface. The high frequency contributions from the outer coordination shells are dra-

matically reduced in EXAFS of the film TF1 deposited on unheated substrate that reflects disappearance of the long-range order in the film, in agreement with XRD data (Fig. 2).

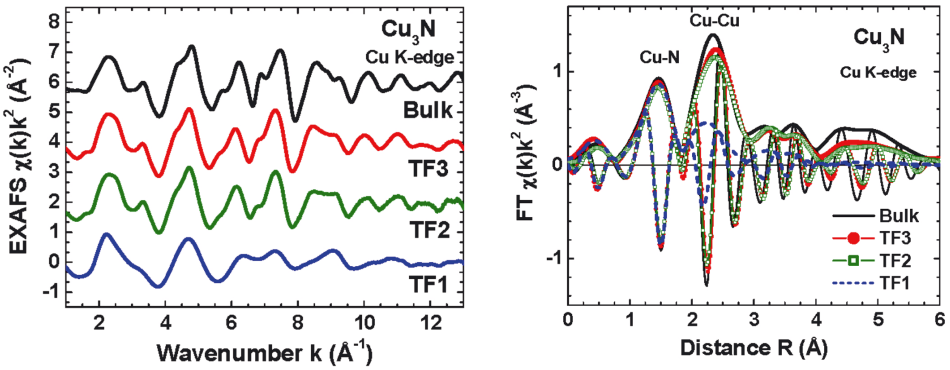

Fig. 4. Experimental Cu K-edge EXAFS $\chi(k)k^2$ and their Fourier transforms (both imaginary parts and moduli are shown) for bulk Cu_3N and thin films.

The values of structural parameters (interatomic distances R and mean-squared relative displacements (MSRD) σ^2) obtained from the analysis of the first two peaks in FTs are reported in Table 2 for bulk Cu_3N and thin films. Note that the coordination numbers (N=2 for Cu–N and N=8 for Cu–Cu) in the films remain as in the bulk within the error of the fit. Also the length of the Cu–N bonds and the MSRD values in all films are close to those in bulk Cu_3N. Moreover, rather small values of the Cu–N MSRDs indicate strong bonding through a mixing of Cu(4s, 4p) states with the Cu(3d)-N(2p) bands estimated by the first principles of electronic structure calculations in [13]. The intensity of the second peak due to the Cu–Cu bonds is reduced in the films due to increasing disorder as is evidenced by the MSRD, whose value increases nearly twice in the amorphous film TF1 compared to bulk Cu_3N.

4. CONCLUSIONS

The atomic structure of copper nitride thin films produced by dc magnetron sputtering was studied by x-ray diffraction and x-ray absorption spectroscopy at the Cu K-edge. We found that the nearest interatomic distance Cu–N in thin films did not change significantly upon substrate heating and was close to that in bulk Cu_3N, indicating strong bonding between copper and nitrogen atoms. At the same time, the second Cu–Cu and outer coordination shells were strongly influenced by structural disorder, which could be reduced by substrate heating during film deposition.

ACKNOWLEDGEMENTS

The present research has been supported by the Latvian National Research Program IMIS2. The EXAFS measurements have been financed from the European Community's Seventh Framework Programme under grant agreement No. 226716 (Project I-20100098 EC).

REFERENCES

1. Zachwieja, U., and Jacobs, H. (1990). Ammonothermalsynthese von kupfernitrid, Cu_3N. *J. Less Common Metals 161*, 175–184. DOI: 10.1016/0022-5088(90)90327-G.
2. Paniconi, G., Stoeva, Z., Doberstein, H., Smith, R. I., Gallagher, B. L., and Gregory, D.H. (2007). Structural chemistry of Cu_3N powders obtained by ammonolysis reactions. *Solid State Sci.* ***9***, 907–913. DOI: 10.1016/j.solidstatesciences.2007.03.017.
3. Asano, M., Umeda, K., and Tasaki, A. (1990). Cu_3N thin film for a new light recording media. *Jpn. J. Appl. Phys. 29*, 1985–1986. DOI: 10.1143/JJAP.29.1985.
4. Maruyama, T., and Morishita, T. (1996). Copper nitride and tin nitride thin films for write-once optical recording media. *Appl. Phys. Lett. 69*, 890–891. DOI: 10.1063/1.117978.
5. Borsa, D.M., Grachev, S., Presura, C., and Boerma, D.O. (2002). Growth and properties of Cu_3N films and Cu_3N/γ'-Fe_4N bilayers. *Appl. Phys. Lett. 80*, 1823–1825. DOI: 10.1063/1.1459116.
6. Wu, H., and Chen, W. (2011). Copper nitride nanocubes: size-controlled synthesis and application as cathode catalyst in alkaline fuel cells. *J. Am. Chem. Soc. 133*, 15236–15239. DOI: 10.1021/ja204748u.
7. Maya, L. (1993). Deposition of crystalline binary nitride films of tin, copper, and nickel by reactive sputtering. *J. Vac. Sci. Technol. A 11*, 604–608. DOI: 10.1116/1.578778.
8. Borsa, D.M., and Boerma, D.O. (2004). Growth, structural and optical properties of Cu_3N films. *Surf. Sci. 548*, 95–105. DOI: 10.1016/j.susc.2003.10.053.
9. Zakutayev, A., Caskey, Ch.M., Fioretti, A.N., Ginley, D.S., Vidal, J., Stevanovic, V., Tea, E., and Lany, S. (2014). Defect tolerant semiconductors for solar energy conversion. *J. Phys. Chem. Lett. 5*, 1117–1125. DOI: 10.1021/jz5001787.
10. Caskey, Ch. M., Richards, R.M., Ginleya, D.S., and Zakutayev, A. (2014). Thin film synthesis and properties of copper nitride, a metastable semiconductor. *Mater. Horiz. 1*, 424–430. DOI: 10.1039/c4mh00049h.
11. Pierson, J.F. (2002). Structure and properties of copper nitride films formed by reactive magnetron sputtering. *Vacuum 66*, 59–64. DOI: 10.1016/S0042-207X(01)00425-0.
12. Maruyama, T., and Morishita, T. (1995). Copper nitride thin films prepared by radio-frequency reactive sputtering. *J. Appl. Phys. 78*, 4104–4107. DOI: 10.1063/1.359868.
13. Hahn, U., and Weber, W. (1996). Electronic structure and chemical-bonding mechanism of Cu_3N, Cu_3NPd, and related Cu(I) compounds. *Phys. Rev. B* ***53***, 12684. DOI: 10.1103/PhysRevB.53.12684.
14. Moreno-Armenta, M.G., Martínez-Ruiz, A., and Takeuchi, N. (2004). Ab initio total energy calculations of copper nitride: The effect of lattice parameters and Cu content in the electronic properties. *Solid State Sci.* 6, 9–14. DOI: 10.1016/j.solidstatesciences.2003.10.014.
15. Hou, Z.F. (2008). Effects of Cu, N, and Li intercalation on the structural stability and electronic structure of cubic Cu_3N. *Solid State Sci.* 10, 1651–1657. DOI: 10.1016/j.solidstatesciences.2008.02.013.
16. Zhao, J.G., Yang, L.X., and Yu, Y., (2006). Pressure-induced metallization and structural evolution of Cu_3N. *Phys. Stat. Sol. (b)* 243, 573–578. DOI: 10.1002/pssb.200541280.
17. Wosylus, A., Schwarz, U., Akselrud, L., Tucker, M.G., Hanfland, M., Rabia, K., Kuntscher, C., von Appen, J., Dronskowski, R., Rau, D., and Niewa, R. (2009). High-pressure phase transition and properties of Cu_3N: An experimental and theoretical study. *Z. Anorg. Allg. Chem.* 635, 1959–1968. DOI: 10.1002/zaac.200900369.

18. Rickers, K., Drube, W., Schulte-Schrepping, H., Welter, E., Brüggmann, U., Herrmann, M., Heuer, J., and Schulz-Ritter, H. (2007). New XAFS Facility for In-Situ Measurements at Beamline C at HASYLAB. A*IP Conf. Proc. 882*, 905–907. DOI: 10.1063/1.2644700
19. Kuzmin, A. (1995). EDA: EXAFS data analysis software package. *Physica B 208-209*, 175–176. DOI: 10.1016/0921-4526(94)00663-G.
20. Aksenov, V.L., Kuzmin, A.Yu., Purans, J., and Tyutyunnikov, S.I. (2006). Development of Methods of EXAFS Spectroscopy on Synchrotron Radiation Beams: Review. *Crystallogr. Rep. 51*, 908–935. DOI: 10.1134/S1063774506060022.
21. Kuzmin, A., and Chaboy, J. (2014). EXAFS and XANES analysis of oxides at the nanoscale. *IUCrJ 1*, 571–589. DOI: 10.1107/S2052252514021101.
22. Ankudinov, A.L., Ravel, B., Rehr, J.J., and Conradson, S.D. (1998). Real-space multiple-scattering calculation and interpretation of x-ray-absorption near-edge structure. *Phys. Rev. B 58*, 7565–7576. DOI: 10.1103/PhysRevB.58.7565.
23. Rehr, J.J., and Albers, R.C. (2000). Theoretical approaches to x-ray absorption fine structure. *Rev. Mod. Phys.* 72, 621–654. DOI: 10.1103/RevModPhys.72.621.
24. Xiao, J., Li, Y., and Jiang, A. (2011). Structure, optical property and thermal stability of copper nitride films prepared by reactive radio frequency magnetron sputtering. *J. Mater. Sci. Technol. 27*, 403–407. DOI: 10.1016/S1005-0302(11)60082-0.
25. Yue, G.H., Yana, P.X., and Wang, J. (2005). Study on the preparation and properties of copper nitride thin films. *J. Crystal Growth 274*, 464–468. DOI: 10.1016/j.jcrysgro.2004.10.032.
26. Kuzmin, A., and Purans, J. (1993). A new fast spherical approximation for calculation of multiple scattering contribution in the X-ray absorption fine structure and its application to ReO_3, $NaWO_3$ and MoO_3. *J. Phys.: Condensed Matter 5*, 267–282. DOI: 10.1088/0953-8984/5/3/004.
27. Anspoks, A., Kalinko, A., Kalendarev, R., and Kuzmin, A. (2012). Atomic structure relaxation in nanocrystalline NiO studied by EXAFS spectroscopy: Role of nickel vacancies. *Phys. Rev. B 86*, 174114, 1–11. DOI: 10.1103/PhysRevB.86.174114.

VARA NITRĪDA PLĀNO KĀRTIŅU STRUKTŪRAS PĒTĪJUMI

A. Kuzmins, A. Kalinko, A. Anspoks,
J. Timošenko, R. Kalendarev

K o p s a v i l k u m s

Šajā darbā mēs ziņojam par vara nitrīda (Cu_3N) plāno kārtiņu rentgendifrakcijas un rentgenabsorbcijas spektroskopijas pētījumu rezultātiem. Teksturētas nanokristāliskās plānās kartiņas tika iegūtas, izmantojot līdzstrāvas magnetrona izputināšanas procesu uz pamatnēm, kas karsētas ap 190°C temperatūrā. Amorfas plānās kārtiņas ar stipri nesakārtotu struktūru jau vara otrajā koordinācijas sfērā tika sagatavotas bez pamatnes karsēšanas.

05.11.2015.